

Investigating Barrow Holographic Dark Energy in Quintessential $f(R, L_m)$ -Gravity with Ricci Scalar as the IR cutoff

G.U. Khapekar, Mohammad Muzammil Mohammad Mukhtar ,
Syed Mudassir Syed Iqbal

Department of Mathematics, Jagadamba Mahavidyalaya and Research Center,
SGB Amravati University, Achalpur City, Maharashtra, India

Received 05 December 2025

Abstract. The current study examines the Barrow Holographic Dark Energy model (BHDE) with the Ricci scalar as the IR cut-off in a flat FLRW line element within the framework of a non-linear $f(R, L_m)$ gravity model. We used $f(R, L_m) = \frac{R}{2} + L_m^n$, where n is a free parameter. Using a Chi-square test and Markov Chain Monte Carlo (MCMC) simulations on Observational Hubble Data (OHD) with 31 points and Pantheon+SHOES data with 1701 points, we find the best match values for model parameters. The best fit ranges for model parameters are as follows: $\eta = 1.3^{+0.08}_{-0.09}$, $H_0 = 65.97^{+2.48}_{-2.42}$ km/s/Mpc for OHD and $\eta = 1.2^{+0.04}_{-0.04}$, $H_0 = 72.77^{+0.24}_{-0.26}$ km/s/Mpc for the Pantheon+SHOES dataset. Our analysis produces a value for H_0 that roughly corresponds with the Planck Collaboration's 2018 estimate of $H_0 = 67.4 \pm 0.5$ km/s/Mpc. Then we examined the behavior of Barrow holographic dark energy density, the equation of state (EoS) parameter and the energy conditions. The equation of state parameter ω in our model reveals that the universe is currently in a quintessence phase. The DEC and WEC confirm the model's credibility due to their positive character. However, the violation of SEC suggests the cosmos is undergoing accelerated expansion. Furthermore, we computed the deceleration parameter q , which indicates a change from a previously decelerating phase to the current phase of accelerating expansion, with $q_0 = -0.35$ (OHD) and $q_0 = -0.4$ (Pantheon+SHOES), implying that the current model is in an accelerating phase. Furthermore, the quintessential behavior of the proposed model is validated through the calculation of the Om diagnostic parameter, jerk parameter, and statefinder parameters. Finally, our model is consistent with recent observational studies, accounts for the current accelerating phase, and is similar to the quintessence dark energy hypothesis.

KEY WORDS: Barrow holographic dark energy, Quintessence, IR cut-off, $f(R, L_m)$ gravity.

1 Introduction

A paradigm shift in our understanding of the cosmos occurred in the late twentieth century. Groundbreaking observations from two independent teams—the High-redshift Supernova Search Team [1] and the Supernova Cosmology Project [2]—provided compelling evidence that our universe is not just expanding but doing so at an accelerating rate. This startling discovery has since been corroborated by a wealth of evidence from diverse cosmological probes, including temperature anisotropies in the Cosmic Microwave Background (CMB) [3–5], the distribution of Large Scale Structures (LSS) [6, 7], and Baryon Acoustic Oscillations (BAO) [8, 9]. Despite this robust observational support, the underlying cause of this late-time cosmic acceleration remains one of the most profound mysteries in modern physics. The prevailing hypothesis attributes this phenomenon to a mysterious component with negative pressure, dubbed dark energy. This enigmatic entity is thought to dominate the universe’s energy budget, constituting approximately 68% of its total density, with dark matter making up about 27% and ordinary baryonic matter a mere 5%. The simplest and most widely accepted framework, the Lambda Cold Dark Matter (Λ CDM) model, identifies dark energy with Einstein’s cosmological constant, Λ [10, 11]. However, this model suffers from significant theoretical challenges, most notably the fine-tuning problem. The theoretical shortcomings of the Λ CDM model have spurred the development of numerous alternative theories, including dynamic dark energy models based on scalar fields (such as quintessence [12, 13], phantom [14], and k-essence [15]) and exotic fluid concepts like the Chaplygin gas [16, 17].

Another compelling avenue of research stems from the holographic principle proposed by G.’t Hooft, a concept originating from black hole physics [18]. This principle posits that the degrees of freedom within a volume of space are encoded on its boundary. Applied to cosmology, this leads to the development of holographic dark energy (HDE) models, which establish a relationship between the short-distance ultraviolet (UV) cutoff and the large-scale infrared (IR) cutoff of the universe. Cohen et al. [19] suggested that, for a system with size L and ultraviolet (UV) cut-off Λ without decaying into a black hole, it is required that the total energy in a region of size L should not exceed the mass of a black hole of the same size, thus $L^3 \rho_\Lambda \leq LM_P^2$. The largest L allowed is the one saturating this inequality; thus, the holographic DE density $\rho_\Lambda = 3c^2 M_P^2 L^{-2}$, where c is a numerical constant and M_P is the reduced Planck mass $M_P^2 = 1/8\pi G$. It means that there must be a duality between UV cut-off and (infra-red) IR cut-off. Therefore, the UV cut-off is related to the vacuum energy and IR cut-off is related to the large scale of the Universe. Hubble’s Horizon [20, 21], event horizon [22], particle horizon [23], conformal universe age [24, 25], Ricci scalar radius [26], Granda-Oliveros cutoff [27] are the examples of infrared cutoffs. However, the original holographic dark energy models [28–30] constructed by

attributing Bekenstein-Hawking entropy and Hubble horizon could not provide a satisfactory explanation for the current accelerated expansion. This has led to models like Tsallis Holographic Dark Energy (THDE) [31] and Rényi Holographic Dark Energy (RHDE) [32]. A particularly intriguing development is the Barrow Holographic Dark Energy (BHDE) model [33] (a detailed explanation is in section 1). IR cutoffs with various HDE models can explain the current state of the universe's accelerated expansion in accordance with current observational data. Recently, Shekh et al. have studied the holographic dark energy with Hubble's and Granda-Oliveros horizon as the infrared cut-off in non-static plane symmetric space-time [34]. Also, the physical acceptability of Renyi, Tsallis and Sharma-Mittal holographic dark energy models in the framework of $f(T, B)$ gravity under Hubble's cutoff was studied by Shekh et al. [35]. Iqbal et al. observed the LRS Bianchi type-I with Hubble's horizon as an IR cut-off in $f(R)$ gravity [36]. Wankhade et al. have studied the cosmos model characterized by LRS Bianchi type-I, where interacting dark matter and the Renyi holographic dark energy model are taken into account within the framework of $f(R)$ gravity [37].

Another way to look beyond dark energy and its models is to change the left-hand side of Einstein's equation, foremost to modified theories of gravity. In order to incorporate these modifications, we can replace the Ricci curvature, represented by R , in the Einstein-Hilbert action with a generic function $f(R)$. This formulation gives rise to the class of theories known as $f(R)$ theories, which have been extensively studied and discussed in the literature [38–40]. Numerous investigations have been conducted on modified theories of gravity that can account for both the early and late-time expansion of the universe. One notable example is the $f(Q)$ gravity, where the Ricci scalar R is replaced by a general function $f(Q)$, with Q representing the non-metricity scalar [41–45]. Other modified theories of gravity, such as $f(T)$ where T represents torsion [46–52], $f(R, G)$ [53, 54], $f(R, T)$ [55–58], and more, provide alternative explanations for the current accelerated expansion of the Universe without invoking an effective DE term, akin to a cosmological constant.

By introducing a direct coupling between the Lagrangian density of matter L_m within the Einstein-Hilbert (EH) action and the generic $f(R)$ function, Bertolami et al. [59] recently introduced a generalized version of modified gravity, specifically the $f(R)$ theory. Expanding on this, Harko and Lobo added arbitrary geometry-matter couplings to the model [60]. Applications in cosmology and astrophysics have been fascinating since non-minimal curvature and matter couplings were introduced into cosmological models [61–63]. Furthermore, the $f(R, L_m)$ gravity, which includes a wide variety of curvature-matter coupling theories, was proposed by Harko and Lobo [64]. Because of the non-vanishing covariant divergence of the energy-momentum tensor in this modified gravity framework, an extra force orthogonal to four velocities emerges. Consequently, the motion of test particles deviates from geodesic paths. Keep in mind that the

$f(R, L_m)$ modified theory of gravity is subject to solar system constraints and does not follow the equivalency principle. tests [65, 66]. The literature on the cosmological implications of the $f(R, L_m)$ gravity theory has grown in recent years due to a surge in interest in the subject [67–69]. Wang and Liao’s recent study [70] examined the energy conditions within the framework of $f(R, L_m)$ gravity. Their research clarified how this modified gravity theory affects energy conditions. Additionally, by including the non-minimal matter-geometry coupling in $f(R, L_m)$ gravity, Goncalves and Moraes [71] performed a cosmological analysis. They investigated how different cosmological phenomena are affected by this coupling. Katore et al. observed dynamics of string cosmological model in $f(R, L_m)$ theory of gravity [72]. Recently, the energy conditions in $f(R, L_m)$ gravity was explored by Wang and Liao [73]. Myrzakulov et al. [74] analyzed observational constraints on freezing quintessence in non-linear $f(R, L_m)$ gravity. Jaybhave et al. have observed the cosmology in $f(R, L_m)$ gravity [75]. Pawde et al. have introduced an anisotropic behavior of the universe in $f(R, L_m)$ gravity with varying deceleration parameter [76]. These studies have yielded important discoveries and offered critical insights into the behavior of gravitational theories that extend beyond general relativity. Inspired by the previous discussion and observations, this article examines Barrow holographic dark energy using the Ricci scalar as an IR cut-off within the framework of $f(R, L_m)$ gravity. The analysis is structured as follows: Section 2 offers a brief mathematical overview of $f(R, L_m)$ gravity. In section 3, we discuss the FLRW metric and cosmic fluid, deriving the field equations for the functional form of $f(R, L_m)$ gravity. Section 4 involves constraining the free parameters with 31 data points from Observational Hubble Data (OHD) and 1701 data points from Pantheon+SHOES. In section 5, we calculate the cosmological parameters by employing Ricci curvature as an IR cut-off in the Barrow holographic dark energy model. Finally, section 6 presents the conclusions summarizing our findings.

2 Overview of $f(R, L_m)$ Gravity

The following action governs the gravitational interactions in $f(R, L_m)$ gravity.

$$S = \int f(R, L_m) \sqrt{-g} d^4x, \quad (1)$$

where $f(R, L_m)$ represents an arbitrary function of the Ricci scalar R , the Lagrangian density of matter term L_m , and g is a determinant of the metric tensor.

The Ricci scalar R can be derived by contracting the Ricci tensor $R_{\mu\nu}$

$$R = g^{\mu\nu} R_{\mu\nu}, \quad (2)$$

where the Ricci tensor is defined by

$$R_{\mu\nu} = \partial_\lambda \Gamma_{\mu\nu}^\lambda - \partial_\mu \Gamma_{\lambda\nu}^\lambda + \Gamma_{\mu\nu}^\lambda \Gamma_{\sigma\lambda}^\sigma - \Gamma_{\nu\sigma}^\lambda \Gamma_{\mu\lambda}^\sigma. \quad (3)$$

Here, $\Gamma_{\beta\gamma}^{\alpha}$ represents the well-known Levi-Civita connection component, given as

$$\Gamma_{\beta\gamma}^{\alpha} = \frac{1}{2}g^{\alpha\lambda}\left(\frac{\partial g_{\gamma\lambda}}{\partial x^{\beta}} + \frac{\partial g_{\lambda\beta}}{\partial x^{\gamma}} - \frac{\partial g_{\beta\gamma}}{\partial x^{\lambda}}\right). \quad (4)$$

Now we can derive the field equation by varying the action integral (1) with respect to the component of metric tensor as given below $g_{\mu\nu}$,

$$f_R R_{\mu\nu} + (g_{\mu\nu}\square - \nabla_{\mu}\nabla_{\nu})f_R - \frac{1}{2}(f - f_{L_m}L_m)g_{\mu\nu} = \frac{1}{2}f_{L_m}T_{\mu\nu}, \quad (5)$$

where, $f_R \equiv \frac{\partial f}{\partial R}$, $f_{L_m} \equiv \frac{\partial f}{\partial L_m}$, $\square \equiv \nabla^{\mu}\nabla_{\mu}$; ∇_{μ} is the covariant derivative and $T_{\mu\nu}$ represents the energy-momentum tensor for matter, given as

$$T_{\mu\nu} = \frac{-2}{\sqrt{-g}} \frac{\delta(\sqrt{-g}L_m)}{\delta g^{\mu\nu}}. \quad (6)$$

The relation between the trace of energy-momentum tensor, Ricci scalar R and the Lagrangian density of matter L_m obtained by contracting the field equation (3)

$$f_R R + 3\square f_R - 2(f - f_{L_m}L_m) = \frac{1}{2}f_{L_m}T, \quad (7)$$

where $\square F = \frac{1}{\sqrt{-g}}\partial_{\alpha}(\sqrt{-g}g^{\alpha\beta}\partial_{\beta}F)$ for any scalar function F . On applying covariant derivative in equation (5), we get

$$\nabla^{\mu}T_{\mu\nu} = 2\nabla^{\mu}\ln f_{L_m}\frac{\partial L_m}{\partial g^{\mu\nu}}. \quad (8)$$

This shows the violation of energy-momentum conservation in $f(R, L_m)$ gravity. Hence, once the nature of the universe under study is known, one can construct viable cosmological models and verify the dynamics of the universe by appropriately choosing the space-time metric.

3 Cosmological Solution Using FLRW Metric

In this article, we investigate the flat FLRW metric, which describes a homogeneous and isotropic universe on a large scale, we assume,

$$ds^2 = dt^2 - a^2(t)[dx^2 + dy^2 + dz^2], \quad (9)$$

where a is the metric potential or the scale factor. The Ricci scalar obtained corresponds to the metric (9) is

$$R = 6\left[\frac{\ddot{a}}{a} + \left(\frac{\dot{a}}{a}\right)^2\right] = 6[2H^2 + \dot{H}], \quad (10)$$

6 Barrow HDE in Quintessential $f(R, L_m)$ -Gravity with Ricci IR cutoff

where H is the Hubble parameter given as $H = \dot{a}/a$, which characterizes the rate of expansion of the universe.

The energy-momentum tensor $T_{\mu\nu}$ characterizing the universe filled with perfect fluid for the Barrow holographic dark energy is given as

$$T_{\mu\nu} = (\rho_B + p)u_\mu u_\nu - pg_{\mu\nu}, \quad (11)$$

where ρ_B and p are the energy density and pressure of Barrow holographic dark energy, respectively. $u^\mu = (0, 0, 0, 1)$ be the four-velocity vector of the fluid, which satisfies the condition $u^\mu u_\mu = 1$.

The field equations that describe the dynamics of the universe in $f(R, L_m)$ gravity is given by using (5), (9) and (11) as,

$$3H^2 f_R + 3H \dot{f}_R + \frac{1}{2}(f - f_R R - f_{L_m} L_m) = \frac{1}{2} f_{L_m} \rho_B \quad (12)$$

and

$$(3H^2 + \dot{H})f_R - 3H \dot{f}_R - \ddot{f}_R + \frac{1}{2}(f - f_{L_m} L_m) = \frac{1}{2} f_{L_m} p, \quad (13)$$

where the dots denote derivatives with respect to cosmic time t . We have the system of two independent field equations (12)-(13) with four unknowns: f , H , ρ_B and p . To study the evolution of the cosmos, we have to completely solve the system using two extra conditions. The conditions are necessary for closing the system and obtaining the unique solution. First, we use the specific functional form of $f(R, L_m)$ gravity, which is expressed as,

$$f(R, L_m) = \frac{R}{2} + L_m^\alpha, \quad (14)$$

where α is constant. The model being taken is influenced by the functional form $f(R, L_m) = f_1(R) + f_2(R)G(L_m)$, which describes the general coupling between matter and geometry [77]. For the non-linear model, we consider $L_m = \rho_B$ [78] for the further calculations.

Using equation (14) in field equations (12) and (13), we have

$$\frac{3}{\alpha \rho_B^{1-\alpha}} H^2 + \frac{(1-\alpha)}{\alpha} \rho_B = \rho_B \quad (15)$$

and

$$\frac{-1}{\alpha \rho_B^{1-\alpha}} (3H^2 + 2\dot{H}) - \frac{(1-\alpha)}{\alpha} \rho_B = p. \quad (16)$$

Now for another condition, we choose the scale factor of the universe, which is crucial in cosmology, particularly for comprehending the fate of the universe

and the dynamics of late time. In this paper, we focus on the special form of the scale factor suggested by [79] and used in [80, 81], which is taken as

$$a(t) = \sqrt[\eta]{\sinh t}, \quad (17)$$

where $\eta > 0$ is an arbitrary constant.

The Hubble parameter acquired by using equation (17) is

$$H(t) = \frac{\coth t}{\eta}. \quad (18)$$

We can reveal the time variable t in terms of redshift z using the relation $a(t) = 1/(1+z)$ that permits a relevant comparison between theoretical data and observations of cosmology. Equation (17) gives

$$t(z) = \sinh^{-1} \left(\left[\frac{1}{1+z} \right]^\eta \right). \quad (19)$$

Now, the Hubble parameter in terms of redshift z obtained by using the equations (18) and (19) is

$$H(z) = \frac{H_0}{\sqrt{2}} [(1+z)^{2\eta} + 1]^{\frac{1}{2}}, \quad (20)$$

where the $H_0 = H(0)$ represents the current value of the Hubble parameter, obtained by putting $z = 0$ in equation (20). Now, we can also replace the differentiation with respect to time by differentiation with respect to redshift, using the relation $\frac{d}{dt} = -(1+z)H(z)\frac{d}{dz}$. Moreover, the dynamics mentioned in equation (20) completely depend on the model's free parameters η and H_0 . In the next section, we constrain these parameters to investigate the cosmological parameters by using convenient observational datasets.

4 Observational Data Analysis

Now, our goal is to limit the free parameters, specifically η and H_0 , via observational data. This method permits us to polish the model by fitting it to observed measurements, thus improving its projecting power and confirming steadiness with present cosmological observations. We have taken a dataset of 31 Observational Hubble Data (OHD) points [82] and 1701 Pantheon+SHOES data points [83, 84] to approximate the free parameters of this model. The details of both datasets are given in the following sections.

4.1 $H(z)$ datasets

Observational Hubble Data (OHD) points yield direct measurements of the Hubble parameter through various redshifts, enabling us to limit model parameters

by fitting to observational data. In this work, we estimated the model parameters η and H_0 using the Chi-square test in conjunction with Markov Chain Monte Carlo (MCMC) simulations. To get the best-fit findings, we used 1000 steps and 100 walkers in our MCMC study. The prior deliveries for the free parameters were preferred as: $\eta \in [0, 2]$ and $H_0 \in [40, 100]$. The Chi-square test is given as

$$\chi_{\text{OHD}}^2(\eta, H_0) = \sum_{i=1}^{31} \left[\frac{H_{\text{obs}}(z_i) - H_{\text{th}}(z_i, \eta, H_0)}{\sigma_H(z_i)} \right]^2. \quad (21)$$

Here, H_{obs} and H_{th} signifies the Hubble parameter's observed and theoretical values (as calculated from the model) respectively. $\sigma_H(z_i)$ reflects the error in measured Hubble parameter $H(z)$ values at each redshift z_i . Using the statistical techniques provided, we found that the best-fit values for our model parameters were $\eta = 1.3_{-0.09}^{+0.08}$ and $H_0 = 65.97_{-2.42}^{+2.48}$ km/s/Mpc. Our research yielded $H_0 = 67.4 \pm 0.5$ km/s/Mpc, which is consistent with the Planck Collaboration's estimate from 2018. Figure 1 shows contour maps of the Hubble dataset's 1- σ and 2- σ confidence regions. Figure 2 shows the error bar plot of 31 points from the Hubble dataset, plotting $H(z)$ against redshift z for our model.

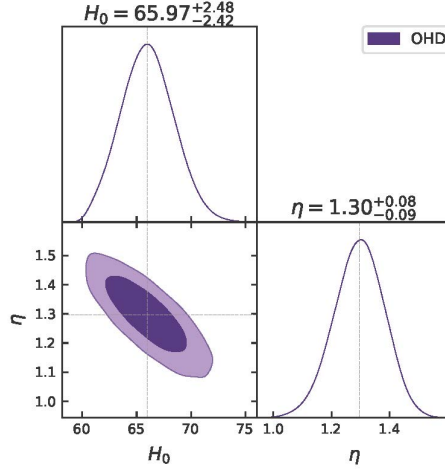


Figure 1. The 1- σ and 2- σ contour maps for parameter η and H_0 using OHD points.

4.2 Pantheon+SHOES datasets

Recently, observations of Type Ia supernovae (SNeIa) have played an important part in proving the universe's accelerating expansion. Among the most prevalent techniques for exploring cosmic acceleration, SNe Ia serve as standardizable candles, allowing for exact measurements of cosmological distances over a wide range of redshifts. Over the past 20 years, the amount and quality of SNe Ia observations have greatly improved, leading to the production of various

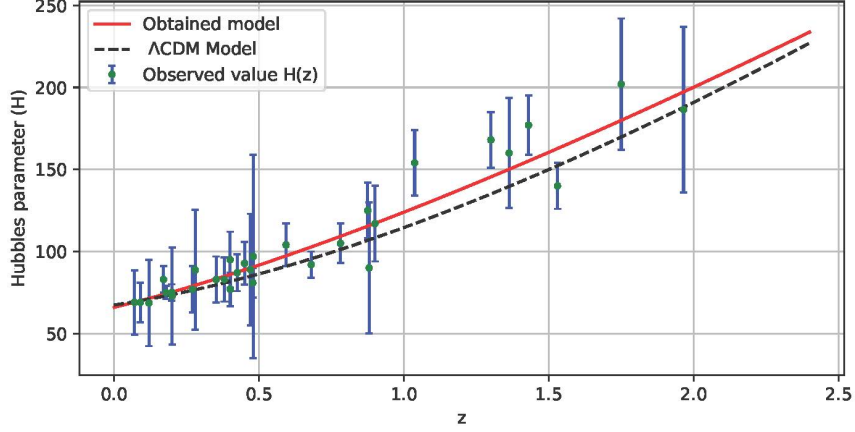


Figure 2. The error bar map utilizing 31 points of OHD together with $H(z)$ versus redshift z for our model is compare with standard Λ CDM model.

comprehensive compilations such as Union, Union 2.1, JLA, Pantheon, and the most recent Pantheon+SHOES sample [85–89]. The Pantheon+SHOES dataset, the most comprehensive and well-curated set of SNe Ia data to date, was also used in this investigation. The 1701 light curves in this sample span a redshift range of $z = 0.00122$ to $z = 2.26137$ and come from 1550 distinct SNe Ia. The theoretical distance modulus μ_i^{th} can be used to express as

$$\mu_i^{\text{th}}(z, \Theta) = 5 \log_{10} d_L(z, \Theta) + 25, \quad (22)$$

where, $\Theta = (\eta, H_0)$ and $d_L(z, \Theta)$ represents the parameter space and the luminosity distance, respectively. Now the luminosity distance is defined as

$$d_L(z, \Theta) = c(z+1) \int_0^z \frac{d\bar{z}}{H(\bar{z})}. \quad (23)$$

Now the chi-square function (χ^2) for the distance modulus for the Pantheon+SHOES dataset is given as

$$\chi^2(z, \Theta) = \sum_{i=1}^{1701} \left[\frac{\mu_{\text{obs}}(z_i) - \mu_{\text{th}}(z_i, \Theta)}{\sigma_{\mu}(z_i)} \right]^2, \quad (24)$$

where the observed and theoretical distance modulus are denoted by μ_{obs} and μ_{th} , respectively. In the meantime, the standard error for the observed distance modulus μ_{obs} is indicated by $\sigma_{\mu}(z_i)$. To maintain consistency, we employed the same number of walkers and steps as in the OHD analysis when running the MCMC procedure for the Pantheon+SHOES dataset. The following is how the previous distributions for the free parameters were chosen. $\eta \in [0, 2]$ and $H_0 \in [40, 100]$. After applying the statistical techniques described, we found the best-fit values

10 Barrow HDE in Quintessential $f(R, L_m)$ -Gravity with Ricci IR cutoff

for our model parameters as $\eta = 1.2_{-0.04}^{+0.04}$, $H_0 = 72.77_{-0.26}^{+0.24}$ km/s/Mpc. Figure 3 shows the contour plots demonstrating the $1-\sigma$ and $2-\sigma$ confidence region for the Pantheon+SHOES dataset. Figure 4 represents the error bar graph, which contains 1701 points of Pantheon+SHOES dataset with $H(z)$ traced against the redshift z

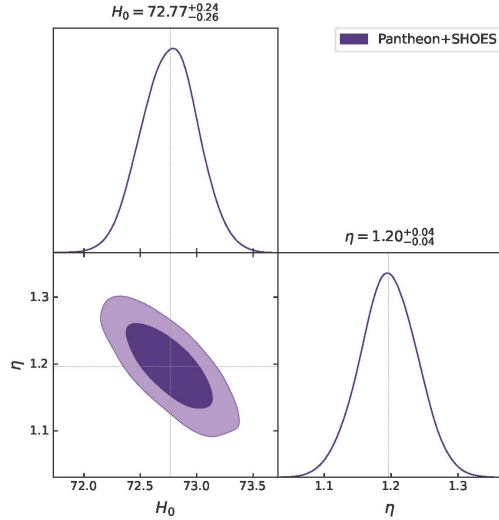


Figure 3. The $1-\sigma$ and $2-\sigma$ contour maps for parameter η and H_0 using Pantheon+SHOES points.

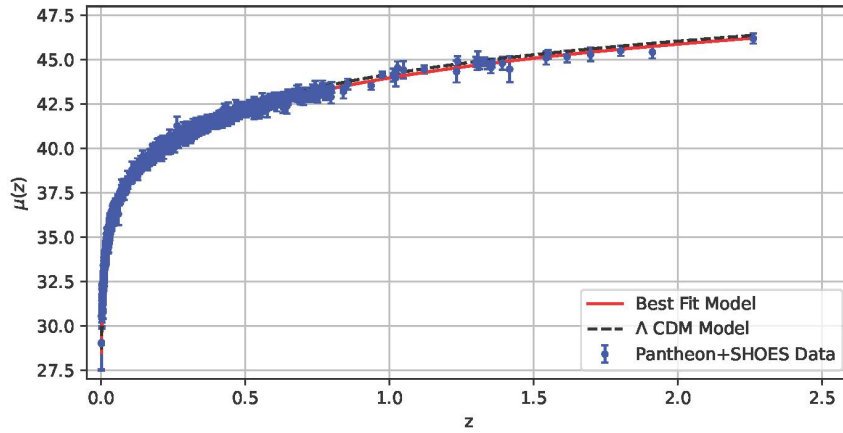


Figure 4. The distance modulus $\mu(z)$ map versus redshift z for our model compared with standard Λ CDM model using 1701 Pantheon+SHOES points.

5 Cosmological parameters using Ricci scalar as IR cut-off

Barrow recently proposed a new black hole entropy relation, which results from the addition of quantum gravitational effects and could have complex fractal features on the black hole region, specifically [90].

$$S_h = \left(\frac{A}{A_0} \right)^{1 + \frac{\Delta}{2}}, \quad (25)$$

where A and A_0 are the area of the black hole horizon and Planck area respectively. Δ be the exponent that computes the extent of quantum-gravitational deformation effects. The new exponent Δ lies in the range $0 \leq \Delta \leq 1$ with $\Delta = 0$ corresponding to the standard smooth structure (in which case Barrow entropy gives back the standard Bekenstein-Hawking ones) and $\Delta = 1$ corresponding to the most intricate structure. The standard holographic dark energy is given by the inequality $\rho L^4 \leq S$, where L is the horizon length, and under the imposition $S \propto A \propto L^2$ [91], the energy density of the Barrow holographic dark energy is expressed as

$$\rho_B = CL^{\Delta-2}, \quad (26)$$

where L can be supposed as the size of the current universe and C is the parameter with dimension $[L]^{2-\Delta}$ and Δ is free parameter. It can be seen that ρ_B reduces to the standard holographic dark energy model $3M_p^2 L^{-2}$ at $\Delta = 0$, where $C = 3M_p^2$. Generally, in the case of the deformation effects produced by Δ when it is not zero, we get the Barrow holographic dark energy that can be distinguished from the standard expression. Currently, Yarahmadi and Muhammad have introduced tilted Barrow interacting holographic dark energy cosmology with Hubble horizon as IR cutoff: a model can alleviate the Hubble and S8 tension [92]. Kotal et al investigated a cosmological parameter analysis and correspondence off $f(R)$, $f(G)$, $f(T)$ gravity models within the (m, n) -type Barrow holographic dark energy framework [93]. Myrzakulov have conducted an investigation into probing dark energy properties with Barrow holographic model in $f(Q, C)$ gravity [94]. Boyar et al. observed Bianchi type VI₀ cosmological model in the context of holographic dark energy in $f(T)$ gravity [95].

The choice of cosmological length L becomes pivotal in establishing the cosmological model. The holographic dark energy models are based on assuming that the energy density is responsible for the current speedup of the universe with L being an appropriate cosmological length. It is well known that the length that plays the role of the IR cutoff on a holographic energy density is not unique. We use the IR cutoff L as Ricci scale $R^{-1/2}$ in our research to find out the Barrow holographic dark energy density [96–98]

$$L = (2H^2 + \dot{H})^{-\frac{1}{2}}. \quad (27)$$

Recently, U. Sharma and V. Srivastava analyzed the Tsallis HDE with an IR cut-off as Ricci horizon in a flat FLRW universe [99]. Observational constraints on Tsallis holographic dark energy with Ricci horizon cutoff was investigated by Zahra Mangoudehi [100]. The holographic induced gravity model with a Ricci dark energy: smoothing the little rip and big rip through Gauss-Bonnet effects was studied by Belkacemi et al. [101]. Interacting Holographic Dark Energy at the Ricci scale and dynamical system was conducted by Mazumdaer et al. [102]. Interacting dark matter and modified holographic Ricci dark energy induce a relaxed Chaplygin gas, which was studied by Chimento et al. [103]. Pawar et al. conducted an analysis of a modified holographic Ricci dark energy model in $f(R, T)$ theory of gravity [104]. Shaikh et al. investigated the hypersurface-homogeneous modified holographic Ricci dark energy cosmological model by hybrid expansion law in Saez-Ballester theory of gravitation [105]. By examining Barrow holographic dark energy density with the Ricci scalar as a potential IR cut-off, we derive cosmological parameters to enhance our comprehension of the current model of the Universe.

5.1 BHDE energy density

Understanding the evolution of the universe requires an understanding of energy density, which influences the formation of galaxies, matter clusters, and the expansion of the universe. In our research, energy density plays a crucial role in elucidating how the universe evolved into its present state. From the equations (20), (26) and (27), it is observed as

$$\rho_B = H_0^{2-\Delta} [\alpha_1(1+z)^{2\eta} + 1]^{1-\frac{\Delta}{2}}, \quad (28)$$

where $\alpha_1 = (2 - \eta)/2$. According to the analysis, the BHDE density stays positive within the range of constrained model parameters, demonstrating compliance with physically realistic conditions. This is important because it shows that the universe has a significant energy density, especially from earlier times. BHDE density decreases as the universe expands because of the dilution of matter over stretching space. Interestingly, from Figure 5, our results for OHD dataset and Pantheon+SHOES dataset indicate that energy density decreases gradually over the evolution of the universe. This suggests that the universe may continue to expand in accordance with the present model.

5.2 Equation of state parameter

The equation of state parameter serves as a crucial tool for pinpointing pivotal moments in the cosmos's evolution, describing the connection between density and pressure. Mathematically, it is expressed as $\omega = p/\rho_B$. It provides a valuable tool for analyzing the dynamics of dark energy and the evolution phases of the universe. When ($\omega > -1$), the universe is in the phantom phase; ($\omega = -1$) corresponds to Λ CDM behavior, while ($-1 < \omega < -1/3$) implying the universe is in the quintessence phase. By solving equations (16), (20) and (28),

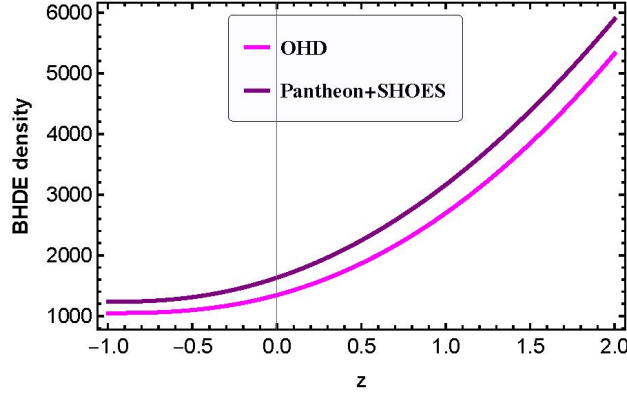


Figure 5. Plot of the Barrow holographic dark energy (BHDE) density versus redshift z .

we derived the equation of state parameter for Barrow holographic dark energy, yielding:

$$\omega = -\frac{1}{\alpha} \left(1 - \alpha + H_0^{\alpha'} \left[\alpha_2(1+z)^{2\eta} + \frac{3}{2} \right] \times \left[\alpha_1(1+z)^{2\eta} + 1 \right]^{\alpha(\frac{\Delta}{2}-1)} \right), \quad (29)$$

where $\alpha' = \alpha(\Delta - 2) + 2$ and $\alpha_2 = (3 - 2\eta)/2$. Figure 6 shows the nature of EoS parameter ω with respect to redshift z (for OHD dataset and Pantheon+SHOES dataset). The study shows that the current behavior of the universe, resembles the quintessence phase. Present values of the equation of state parameter being $\omega_0 = -0.5951$ and $\omega_0 = -0.6058$ for OHD dataset and Pantheon+SHOES dataset respectively, indicating an ongoing accelerating phase of the universe.

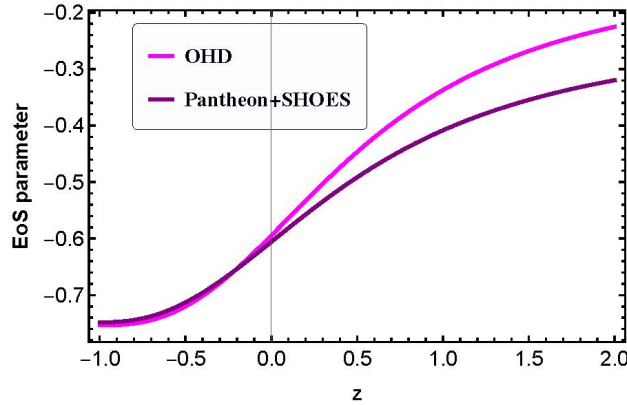


Figure 6. Plot of the Equation of state (EoS) parameter versus redshift z .

5.3 Energy conditions

The energy conditions establish linear correlations between energy density and pressure, as originally derived by Raychaudhuri [106, 107]. These conditions are essential for assessing dark energy models and play a key role in confirming the universe's accelerated expansion. This study concentrates on three significant energy conditions: the null energy condition (NEC), the dominant energy condition (DEC), and the strong energy condition (SEC). Analyzing these conditions imposes constraints that enhance our understanding of the dynamics and features of the model in question. They are defined as follows:

- Null energy condition: $\rho_B + p$.
- Dominating energy condition: $\rho_B - p$.
- Strong energy condition: $\rho_B + 3p$

From equations (16), (20) and (28) the energy conditions in our model can be expressed as,

$$\rho_B + p = \frac{1}{\alpha} H_0^{2-\Delta} [\alpha_1(1+z)^{2\eta} + 1]^{1-\frac{\Delta}{2}} \times \left(2\alpha - 1 - H_0^{\alpha'} [\alpha_2(1+z)^{2\eta} + \frac{3}{2}] [\alpha_1(1+z)^{2\eta} + 1]^{\alpha(\frac{\Delta}{2}-1)} \right), \quad (30)$$

$$\rho_B - p = \frac{1}{\alpha} H_0^{2-\Delta} [\alpha_1(1+z)^{2\eta} + 1]^{1-\frac{\Delta}{2}} \times \left(1 + H_0^{\alpha'} [\alpha_2(1+z)^{2\eta} + \frac{3}{2}] [\alpha_1(1+z)^{2\eta} + 1]^{\alpha(\frac{\Delta}{2}-1)} \right), \quad (31)$$

$$\rho_B + 3p = \frac{1}{\alpha} H_0^{2-\Delta} [\alpha_1(1+z)^{2\eta} + 1]^{1-\frac{\Delta}{2}} \times \left(4\alpha - 3 - H_0^{\alpha'} [\alpha_2(1+z)^{2\eta} + \frac{3}{2}] [\alpha_1(1+z)^{2\eta} + 1]^{\alpha(\frac{\Delta}{2}-1)} \right). \quad (32)$$

Figures 7, 8 and 9 represents the energy conditions for OHD dataset and Pantheon+SHOES dataset, as a function of redshift z . In the present study, it is

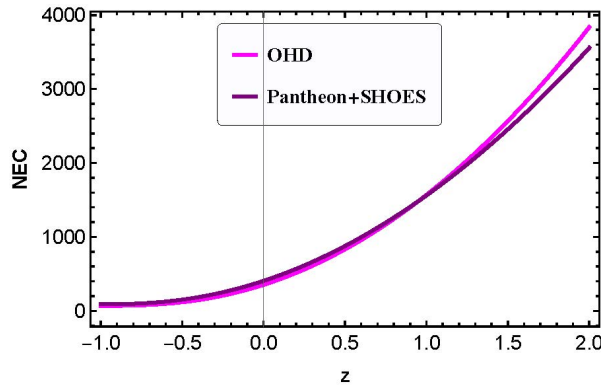
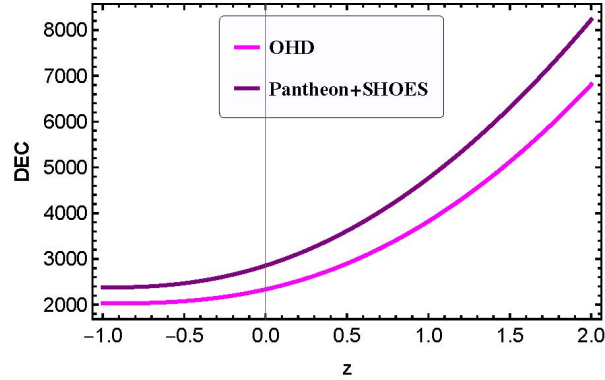
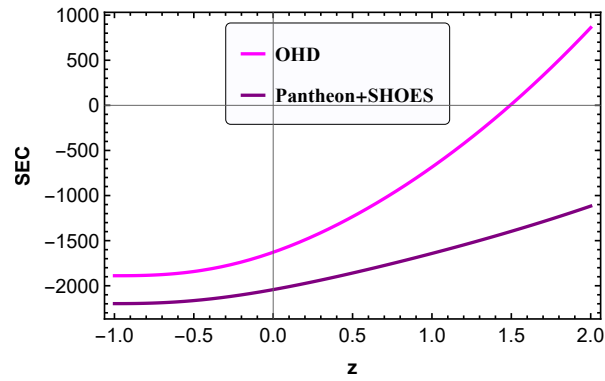


Figure 7. Plot of the Null energy condition (NEC) verses redshift z .

Figure 8. Plot of the Dominant energy condition (DEC) versus redshift z .Figure 9. Plot of the Strong energy condition (SEC) versus redshift z .

noticed that NEC and DEC are satisfied throughout the cosmic evolution, while it is important to highlight that SEC is violated, and this violation is attributed to the accelerating expansion of the universe.

5.4 Deceleration parameter

A pivotal cosmological metric instrumental in discerning whether the universe's expansion is decelerating or accelerating is the deceleration parameter, denoted as q . A positive value of q denotes a decelerating expansion, whereas a negative value signifies an accelerating expansion. Furthermore, the deceleration parameter offers valuable insights into the dynamics and evolutionary trajectory of the universe. The parameter q can be mathematically formulated in relation to the Hubble parameter H , with a dependency on the redshift z , as elucidated by the work of Xu et al. [108]. The deceleration parameter, which describes the

dynamics of the expansion of universe, is given as

$$q(z) = -1 - \frac{\dot{H}}{H^2}. \quad (33)$$

Now, using equation (20) in equation (33) gives

$$q(z) = -1 + \frac{\eta(1+z)^{2\eta}}{1+(1+z)^{2\eta}}. \quad (34)$$

The behavior of the deceleration parameter versus the redshift z is shown in Figure 10. The shift in the universe's expansion from a decelerating phase to an accelerating one is evident in Figure 10. Moreover, the present values of the deceleration parameter are about $q_0 = -0.35$ (OHD) and $q_0 = -0.4$ (Pantheon+SHOES), with a transition redshift of near $z_t = 0.588$ (OHD) and $z_t = 0.955$ (Pantheon+SHOES).

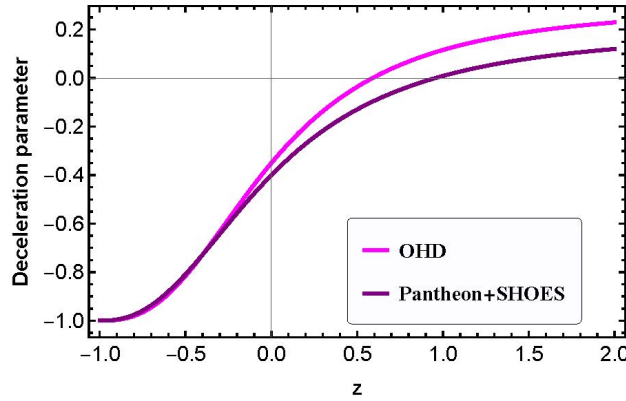


Figure 10. Plot of the deceleration parameter (q) versus redshift z .

5.5 Om diagnostic parameter

The $Om(z)$ diagnostic introduced by Sahni et al. is a geometric tool designed to understand the dynamic characteristics of dark energy cosmological models grounded on the slope of the diagnostic plot. The negative slope advocates a quintessence behavior, with the equation of state parameter $\omega > -1$. On the other hand, a positive slope of $Om(z)$ specifies a phantom behavior for the model, which resembles an equation of state parameter $\omega < -1$. While the dark energy model acts like a cosmological constant Λ CDM if the slope remains constant with respect to redshift z . For a universe that is spatially flat, the $Om(z)$ diagnostic can be expressed in terms of the Hubble parameter H and the cosmo-

logical redshift z as follows:

$$Om(z) = \frac{\left(\frac{H(z)}{H_0}\right)^2 - 1}{(1+z)^3 - 1}, \quad (35)$$

where H_0 be the present Hubble constant. The $Om(z)$ diagnostic for this model is as follows from equation (20) and equation (35), we get

$$Om(z) = \frac{(1+z)^{2\eta} + 1}{(1+z)^3 - 1}. \quad (36)$$

Figure 11 demonstrates the evolution of the $Om(z)$ diagnostic parameter in this model using the OHD and Pantheon+SHOES datasets. The negative slope witnessed in $Om(z)$ points to a quintessence behavior exhibited by this model, reliable with a dynamical dark energy component that efforts the accelerated expansion of the universe.

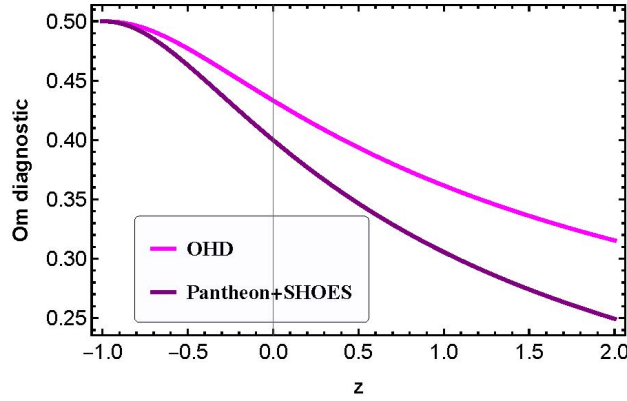


Figure 11. Plot of the Om diagnostic parameter verses redshift z .

5.6 Jerk parameter

The Jerk parameter is vital to defining the dynamics of the universe. The benefit of this parameter is that it gives the idea of the current phase of the universe as well as transitions from the decelerating phase to the accelerating phase. The value of the jerk parameter $j = 1$ resembles the flat Λ CDM model, a negative value of the jerk parameter describes the decelerating phase, and a positive value denotes the accelerating phase. The jerk parameter is given by

$$j = 1 - 2(1+z) \frac{H'(z)}{H(z)} + (1+z)^2 \left[\frac{H''(z)}{H(z)} + \left(\frac{H'(z)}{H(z)} \right)^2 \right]. \quad (37)$$

Utilizing equation (20) and Figure 12 illustrates that the jerk parameter j remains positive all over the progression of the universe (for OHD dataset and Pantheon+SHOES dataset), which shows the universe is in an accelerating phase. In the far future ($z \rightarrow -1$), the jerk parameter tends to 1, which shows the present model to be similar to the Λ CDM model.

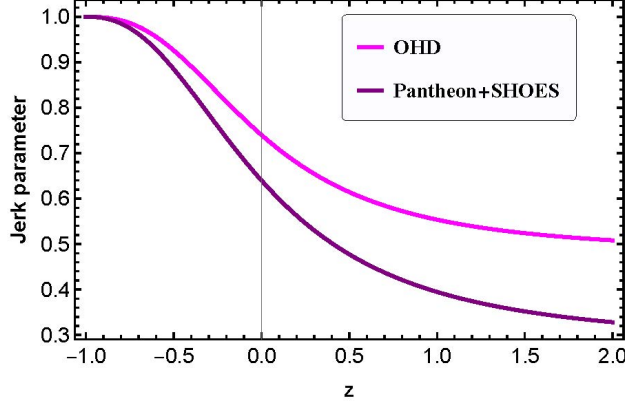


Figure 12. Plot of the jerk parameter j versus redshift z .

5.7 Statefinder parameters

The statefinder parameters play an important role in clarifying the accelerated expansion of the universe and understanding the nature of dark energy. As various dark energy models have been proposed, to differentiate between these models, the parameter used is known as the statefinder parameters. It is related to the third derivative of the scale factor and was introduced by Sahni et al. The statefinder parameters denote various dark energy models for distinct values of (r, s) , such as

- $(r = 1, s = 0) \implies \Lambda$ CDM model,
- $(r = 1, s = 1) \implies$ SCDM model,
- $(r > 1, s < 0) \implies$ Chaplygin gas model,
- $(r < 1, s > 0) \implies$ Quintessence model.

The statefinder parameters (r, s) are given as

$$r = 1 - 2(1+z)\frac{H'(z)}{H(z)} + (1+z)^2 \left[\frac{H''(z)}{H(z)} + \left(\frac{H'(z)}{H(z)} \right)^2 \right], \quad (38)$$

$$s = \frac{r-1}{3(q-\frac{1}{2})}. \quad (39)$$

Using equation (20) in equation (38) yields

$$r = 1 - \frac{\eta[3 - 2\eta](1 + z)^{2\eta}}{1 + (1 + z)^{2\eta}}. \quad (40)$$

Now utilizing equation (20), (40) in equation (39) results

$$s = \frac{2\eta[2\eta - 3](1 + z)^{2\eta}}{3[(2\eta - 3)(1 + z)^{2\eta} - 3]}. \quad (41)$$

From Figures 13 and 14, it is clear that the model is in the Quintessence region at the present ($z = 0$) and it goes to the Λ CDM model in the far future ($z \rightarrow -1$). For both of the datasets used, the present model is in the quintessence phase, which describes the accelerated expansion of the universe.

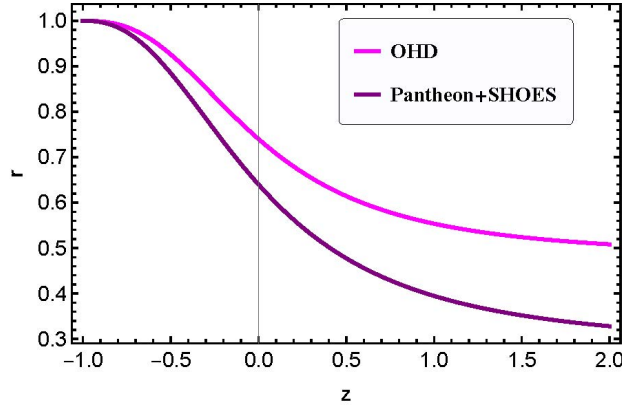


Figure 13. Plot of the statefinder parameter r versus redshift z .

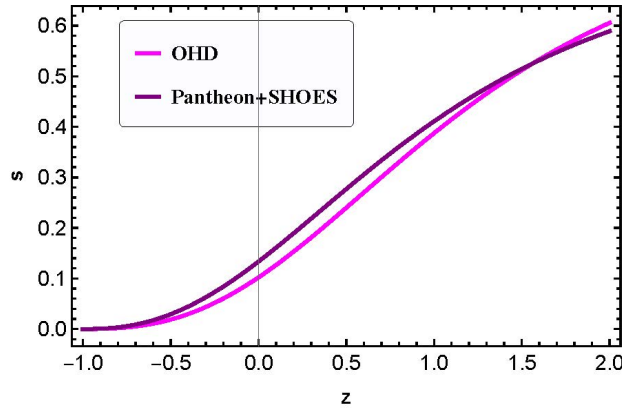


Figure 14. Plot of the statefinder parameter s versus redshift z .

6 Conclusions

This study examined the Barrow holographic dark energy model in FLRW space-time using the Ricci scalar as the candidate for the infrared cutoff, taking into account of the $f(R, L_m)$ -gravity framework. We began by briefly outlining the theory's mathematical formulation. The field equations for the flat FLRW metric were derived by assuming that the Barrow holographic dark energy's content is a perfect fluid. After that, we consider some conditions to solve the field equation. Firstly, a non-linear function $f(R, L_m) = R/2 + L_m^n$, where n is a free parameter. To derive results from the field equations, we assumed a hyperbolic scale factor $a(t) = \sqrt[n]{\sinh t}$, where $\eta > 0$ is an arbitrary constant. Then we productively constraint free parameters by using Observational Hubble dataset (OHD) and Pantheon+SHOES dataset. We used the optimal values for free parameters as $\alpha = 1.24$ and $\Delta = 0.34$, achieving results that are well align with observational data. The best-fit values were found to be $\eta = 1.3^{+0.08}_{-0.09}$ and $H_0 = 65.97^{+2.48}_{-2.42}$ km/s/Mpc for the OHD dataset, and $\eta = 1.2^{+0.04}_{-0.04}$ and $H_0 = 72.77^{+0.24}_{-0.26}$ km/s/Mpc for the Pantheon+SHOES dataset. The obtained value of H_0 is in good agreement with the Planck Collaboration's 2018 value of $H_0 = 67.4 \pm 0.5$ km/s/Mpc.

In this study we have expressed different important cosmological parameters like Barrow holographic dark energy (BHDE), Equation of state (EoS) parameter, Energy conditions, deceleration parameter, Om diagnostic parameter and statefinder parameters in terms of redshift z and to improve our understanding of the present model. The Barrow holographic dark energy density ρ_B is overall positive throughout the evolution of the universe which is necessary for the physical viability of our model. Also, the evolution of equation of state parameter demonstrates that the current nature of the universe in our model resembles a quintessence phase with present values of the equation of state parameter being $\omega_0 = -0.5951$ and $\omega_0 = -0.6058$ for OHD dataset and Pantheon+SHOES dataset respectively, resembling a current accelerated expansion. Furthermore, we determine prominent energy conditions like NEC, DEC, and SEC for this study. We investigate that NEC and DEC are satisfied throughout the cosmic evolution. But the violation of SEC resembles the current observations and shows an accelerating phase of the universe. Moreover, The deceleration parameter $q(z)$ indicated a shift from a decelerating to an accelerating expansion phase, with current values of $q = -0.35$ based on OHD and $q = -0.4$ from Pantheon+SHOES. The redshift transitions were determined to be $z_t = 0.5951$ for OHD and $z_t = 0.9594$ for Pantheon+SHOES, aligning with observational data. Additionally, the behavior of the $Om(z)$ diagnostic parameter suggested a quintessence phase for our model, as it exhibited a negative slope, which is consistent with a dynamic dark energy component that efforts the accelerated expansion of the universe. Furthermore, the jerk parameter j remains positive in the overall progression of the universe, showing the accelerated expansion of

the universe. Finally, the statefinder (r, s) parameters illustrate that our model is in quintessence phase and will achieve standard Λ CDM model in the far future ($z \rightarrow -1$). The discussion above leads to the conclusion that our model indicates the quintessential behavior, i.e., an accelerated expansion phase, aligning well with the recent observations.

References

- [1] A.G. Riess, A.V. Filippenko, P. Challis, A. Clocchiatti, A. Diercks, P.M. Garnavich, R.L. Gilliland, C.J. Hogan, S. Jha, R.P. Kirshner, et al. (1998) Observational evidence from supernovae for an accelerating universe and a cosmological constant. *Astron. J.* **116**(3) 1009.
- [2] S. Perlmutter, G. Aldering, G. Goldhaber, R.A. Knop, P. Nugent, P.G. Castro, S. Deustua, S. Fabbro, A. Goobar, D.E. Groom, et al. (1999) Measurements of w and Λ from 42 high-redshift supernovae. *Astrophys. J.* **517**(2) 565.
- [3] D.N. Spergel, L. Verde, H.V. Peiris, E. Komatsu, M. Nolta, C.L. Bennett, M. Halpern, G. Hinshaw, N. Jarosik, A. Kogut, et al. (2003) First-year Wilkinson microwave anisotropy probe (WMAP)* observations: determination of cosmological parameters, *Astrophys. J. Suppl. Series* **148**(1) 175.
- [4] D.N. Spergel, R. Bean, O. Doré, M. Nolta, C. Bennett, J. Dunkley, G. Hinshaw, N.E. Jarosik, E. Komatsu, L. Page, et al. (2007) Three-year Wilkinson microwave anisotropy probe (WMAP) observations: implications for cosmology. *Astrophys. J. Suppl. Series* **170**(2) 377.
- [5] E. Komatsu, J. Dunkley, M. Nolta, C.L. Bennett, B. Gold, G. Hinshaw, N. Jarosik, D. Larson, M. Limon, L. Page, et al. (2009) Five-year Wilkinson microwave anisotropy probe* observations: cosmological interpretation. *Astrophys. J. Suppl. Series* **180**(2) 330.
- [6] M. Tegmark, M. A. Strauss, M.R. Blanton, K. Abazajian, S. Dodelson, H. Sandvik, X. Wang, D.H. Weinberg, I. Zehavi, N.A. Bahcall, et al. (2004) Cosmological parameters from SDSS and WMAP. *Phys. Rev. D* **69**(10) 103501.
- [7] M. Tegmark, D.J. Eisenstein, M.A. Strauss, D.H. Weinberg, M.R. Blanton, J.A. Frieman, M. Fukugita, J.E. Gunn, A.J. Hamilton, G.R. Knapp, et al. (2006) Cosmological constraints from the SDSS luminous red galaxies. *Phys. Rev. D* **74**(12) 123507.
- [8] W.J. Percival, B.A. Reid, D.J. Eisenstein, N.A. Bahcall, T. Budavari, J.A. Frieman, M. Fukugita, J.E. Gunn, Z. Ivezić, G.R. Knapp, et al. (2010) Baryon acoustic oscillations in the sloan digital sky survey data release 7 galaxy sample. *MNRAS* **401**(4) 2148-2168.
- [9] D.J. Eisenstein, I. Zehavi, D.W. Hogg, R. Scoccimarro, M.R. Blanton, R.C. Nichol, R. Scranton, H.-J. Seo, M. Tegmark, Z. Zheng, et al. (2005) Detection of the baryon acoustic peak in the large-scale correlation function of sdss luminous red galaxies. *Astrophys. J.* **633**(2) 560.
- [10] P.J.E. Peebles, B. Ratra (2003) The cosmological constant and dark energy. *Rev. Mod. Phys.* **75**(2) 559.
- [11] M. Miville-Deschênes, V. Pettorino, M. Bucher, J. Delabrouille, K. Ganga, M. Le Jeune, G. Patanchon, C. Rosset, G. Roudier, Y. Fantaye, et al. (2020) Planck 2018 results: VI. Cosmological parameters. *Astron. Astrophys.* **641** A6-A6.

- [12] S.M. Carroll (1998) Quintessence and the rest of the world: suppressing long-range interactions. *Phys. Rev. Lett.* **81**(15) 3067.
- [13] A. Pradhan, A. Dixit, D.C. Maurya (2022) Quintessence behavior of an anisotropic bulk viscous cosmological model in modified $f(Q)$ gravity. *Symmetry* **14**(12) 2630.
- [14] R.R. Caldwell (2002) A phantom menace? Cosmological consequences of a dark energy component with super-negative equation of state. *Phys. Lett. B* **545**(1-2) 23-29.
- [15] R. Myrzakulov (2012) Cosmology of $f(T)$ gravity and k-essence. *Entropy* **14**(9) 1627-1651.
- [16] M.C. Bento, O. Bertolami, A.A. Sen (2002) Generalized Chaplygin gas, accelerated expansion, and dark-energy-matter unification. *Phys. Rev. D* **66**(4) 043507.
- [17] G.N. Gadbail, S.Arora, P. Sahoo (2023) Cosmology with viscous generalized Chaplygin gas in $f(Q)$ gravity. *Ann. Phys. (N. Y.)* **451** 169269.
- [18] G. 't Hooft (1993) Dimensional reduction in quantum gravity. [arXiv preprint gr-qc/9310026](https://arxiv.org/abs/gr-qc/9310026).
- [19] A.G. Cohen, D.B. Kaplan, A.E. Nelson (1999) Effective field theory, black holes, and the cosmological constant. *Phys. Rev. Lett.* **82**(25) 4971.
- [20] L. Xu (2009) Holographic dark energy model with Hubble horizon as an IR cut-off. *J. Cosmol. Astropart. Phys.* **2009**(09) 016.
- [21] J. Liu, Y. Gong, X. Chen (2010) Dynamical behavior of the extended holographic dark energy with the Hubble horizon. *Phys. Rev. D* **81**(8) 083536.
- [22] Y. Nomura, G.N. Remmen (2018) Area law unification and the holographic event horizon. *JHEP* **63**(8) 1-34.
- [23] H.M. Sadjadi (2007) The particle versus the future event horizon in an interacting holographic dark energy model. *J. Cosmol. Astropart. Phys.* **2007**(02) 026.
- [24] Z.-P. Huang, Y.-L. Wu (2012) Holographic dark energy model characterized by the conformal-age-like length. *Int. J. Mod. Phys. A* **27**(16) 1250085.
- [25] Z.-P. Huang, Y.-L. Wu (2012) Cosmological constraint and analysis on holographic dark energy model characterized by the conformal-age-like length. *Int. J. Mod. Phys. A* **27**(22) 1250130.
- [26] E.-K. Li, Y. Zhang, J.-L. Geng, P.-F. Duan (2015) Generalized holographic Ricci dark energy and generalized second law of thermodynamics in Bianchi type I universe. *Gen. Relativ. Gravit.* **47** 1-13.
- [27] A. Khodam-Mohammadi, A. Pasqua, M. Malekjani, I. Khomenko, M. Monshizadeh (2013) Statefinder diagnostic of logarithmic entropy corrected holographic dark energy with granda-oliveros IR cut-off. *Astrophys. Space Sci.* **345**(2) 415-420.
- [28] P. Hořava, D. Minic (2000) Probable values of the cosmological constant in a holographic theory. *Phys. Rev. Lett.* **85**(8) 1610.
- [29] S.D. Hsu (2004) Entropy bounds and dark energy. *Phys. Lett. B* **594**(1-2) 13-16.
- [30] M. Li (2004) A model of holographic dark energy. *Phys. Lett. B* **603**(1-2) 1-5.
- [31] M. Tavayef, A. Sheykhi, K. Bamba, H. Moradpour (2018) Tsallis holographic dark energy. *Phys. Lett.s B* **781** 195-200.
- [32] H. Moradpour, S. Moosavi, I. Lobo, J.M. Graça, A. Jawad, I. Salako (2018) Thermodynamic approach to holographic dark energy and the Rényi entropy. *Eur. Phys. J. C* **78** 1-6.

- [33] S. Nojiri, S.D. Odintsov, T. Paul (2022) Barrow entropic dark energy: A member of generalized holographic dark energy family. *Phys. Lett. B* **825** 136844.
- [34] S. Shekh, M. Muzammil, R. Mapari, G. Khapekar, A. Dixit (2023) Exploring holographic dark energy with Hubble's and Granda-Oliveros horizons as the infrared cut-off in non-static plane symmetric space-time. *Int. J. Geom. Methods Mod. Phys.* **20**(13) 2350233.
- [35] S.H. Shekh, P.H. Moraes, P.K. Sahoo (2021) Physical acceptability of the Renyi, Tsallis and Sharma-Mittal holographic dark energy models in the $f(T, B)$ gravity under Hubble's cutoff. *Universe* **7**(3) 67.
- [36] S.M.S. Iqbal, G. Khapekar, S. Shekh, A. Dixit (2024) LRS Bianchi type-I with Hubble's horizon as IR cut-off in $f(R)$ gravity. *New Astronomy* **113** 102274.
- [37] K.S. Wankhade, A. Shaikh, S.N. Khan (2023) Renyi holographic dark energy model in $f(R)$ gravity with Hubble's IR cut-off. *East Eur. J. Phys.* **3** 87-95.
- [38] H.A. Buchdahl (1970) Non-linear lagrangians and cosmological theory. *MNRAS* **150**(1) 1-8.
- [39] R. Kerner (1982) Cosmology without singularity and nonlinear gravitational Lagrangians. *Gen. Relativ. Grav.* **14** 453-469.
- [40] H. Kleinert, H.-J. Schmidt (2002) Cosmology with curvature-saturated gravitational lagrangian $R/\sqrt{1+l^4/R^2}$. *Gen. Relativ. Grav.* **34**(8) 1295-1318.
- [41] J.B. Jiménez, L. Heisenberg, T. Koivisto (2018) Coincident general relativity. *Phys. Rev. D* **98**(4) 044048.
- [42] J.B. Jiménez, L. Heisenberg, T. Koivisto, S. Pekar (2020) Cosmology in $f(q)$ geometry. *Phys. Rev. D* **101**(10) 103507.
- [43] S.M. Syed Iqbal, G. Khapekar, S. Bhojar (2025) Study of non-static plane symmetric universe with exponential scale factor and perfect fluid in $f(q)$ -gravity. *Int. J. Theor. Phys.* **64**(4) 96.
- [44] S. Shekh, A. Pradhan, G. Khapekar, S.M.S. Iqbal (2024) Quintessence dark energy non-static plane symmetric universe in $f(q)$ theory of gravity. *Indian J. Phys.* 1-15.
- [45] S.M.S. Iqbal, G. Khapekar (2025) Exploring the evolution of a non-static plane symmetric universe with cosmic strings and LVDP in $f(q)$ gravity. *New Astronomy* 102455.
- [46] S. Capozziello, V. Cardone, H. Farajollahi, A. Ravanpak (2011) Cosmography in $f(t)$ gravity *Phys. Rev. D* **84**(4) 043527.
- [47] D. Liu, M. Reboucas (2012) Energy conditions bounds on $f(t)$ gravity. *Phys. Rev. D* **86**(8) 083515.
- [48] L. Iorio, E.N. Saridakis (2012) Solar system constraints on $f(t)$ gravity, *MNRAS* **427**(2) 1555-1561.
- [49] D. Wang, D. Mota (2020) Can $f(t)$ gravity resolve the H_0 tension? *Phys. Rev. D* **102**(6) 063530.
- [50] R.C. Nunes, S. Pan, E.N. Saridakis (2016) New observational constraints on $f(t)$ gravity from cosmic chronometers. *J. Cosmol. Astropart. Phys.* **2016**(08) 011.
- [51] S.M.S. Iqbal, G. Khapekar (2025) Exploring cosmological effects of a constant jerk parameter in flrw universe within $f(t)$ gravity. *Astrophys. Space Sci.* **370**(4) 38.
- [52] S.M. Iqbal, G. Khapekar (2024) Analyzing the Bianchi type-I universe with a special form of deceleration parameter in $f(t)$ gravity. *Prespacetime Journal* **15**(4) .

- [53] S. Shekh, S. Arora, V. Chirde, P. Sahoo (2020) Thermodynamical aspects of relativistic hydrodynamics in $f(r, g)$ gravity. *Int. J. Geom. Methods Mod. Phys.* **17**(03) 2050048.
- [54] S. Shekh (2021) Dynamical analysis with thermodynamic aspects of anisotropic dark energy bounce cosmological model in $f(r, g)$ gravity. *New Astronomy* **83** 101464.
- [55] T. Harko, F.S. Lobo, S. Nojiri, S.D. Odintsov (2011) $f(r, t)$ gravity. *Phys. Rev. D* **84**(2) 024020.
- [56] P. Sahoo, B. Mishra, G. Chakradhar Reddy (2014) Axially symmetric cosmological model in $f(r, t)$ gravity. *Eur. Phys. J. Plus* **129** 1-8.
- [57] V. Patil, P. Bolke, S. Waghmare, J. Pawde (2023) Energy conditions and statefinder diagnostic of cosmological model with special law of Hubble parameter in $f(r, t)$ gravity. *East Eur. J. Phys.* 53-61.
- [58] V. Dagwal, D. Pawar, Y. Solanke (2020) Study of cosmic models in $f(r, t)$ gravity with tilted observers. *Mod. Phys. Lett. A* **35**(38) 2050316.
- [59] O. Bertolami, C.G. Boehmer, T. Harko, F.S. Lobo (2007) Extra force in $f(r)$ modified theories of gravity. *Phys. Rev. D* **75**(10) 104016.
- [60] T. Harko (2008) Modified gravity with arbitrary coupling between matter and geometry. *Phys. Lett. B* **669**(5) 376-379.
- [61] T. Harko (2010) Galactic rotation curves in modified gravity with nonminimal coupling between matter and geometry. *Phys. Rev. D* **81**(8) 084050.
- [62] T. Harko (2010) The matter lagrangian and the energy-momentum tensor in modified gravity with nonminimal coupling between matter and geometry. *Phys. Rev. D* **81**(4) 044021.
- [63] V. Faraoni (2007) Viability criterion for modified gravity with an extra force. *Phys. Rev. D* **76**(12) 127501.
- [64] T. Harko, F.S. Lobo (2010) $f(r, 1m)$ gravity. *Eur. Phys. J. C* **70** 373-379.
- [65] V. Faraoni, V. Faraoni (2004) *Scalar-Tensor Gravity*. Springer.
- [66] O. Bertolami, J. Páramos, S.G. Turyshev (2008) General theory of relativity: Will it survive the next decade? in: *Lasers, Clocks and Drag-Free Control: Exploration of Relativistic Gravity in Space*. Springer, pp. 27-74.
- [67] G. Carvalho, R. Lobato, D. Deb, P. Moraes, M. Malheiro (2022) Quark stars with 2.6 m in a non-minimal geometry-matter coupling theory of gravity. *Eur. Phys. J. C* **82**(12) 1096.
- [68] R. Lobato, G. Carvalho, C. Bertulani (2021) Neutron stars in $f(R, L_m)$ gravity with realistic equations of state: joint-constrains with GW170817, massive pulsars, and the PSR J0030+ 0451 mass-radius from nicer data. *Eur. Phys. J. C* **81**(11) 1-7.
- [69] T. Harko, S. Shahidi (2022) Palatini formulation of the conformally invariant $f(R, L_m)$ gravity theory. *Eur. Phys. J. C* **82**(11) 1003.
- [70] J. Wang, K. Liao (2012) Energy conditions in $f(R, L_m)$ gravity, *Class. Quantum Grav.* **29**(21) 215016.
- [71] B. Goncalves, P. Moraes, B. Mishra (2023) Cosmology from non-minimal geometry-matter coupling. *Fortschritte der Physik* **71**(8-9) 2200153.
- [72] S. Katore, P. Agrawal, H. Paralikar, A. Nile (2025) Dynamics of string cosmological model in $f(R, L_m)$ theory of gravity. *East Eur. J. Phys.* 1 70-78.

- [73] J. Wang, K. Liao (2012) Energy conditions in $f(R, L_m)$ gravity. *Class. Quantum Grav.* **29**(21) 215016.
- [74] Y. Myrzakulov, M. Koussour, A. Caliskan, E. Güdekli, S. Muminov, J. Rayimbaev (2024) Observational constraints on freezing quintessence in a non-linear $f(R, L_m)$ gravity. *arXiv:2412.10518*.
- [75] L.V. Jaybhaye, R. Solanki, S. Mandal, P. Sahoo (2022) Cosmology in $f(R, L_m)$ gravity. *Phys. Lett. B* **831** 137148.
- [76] J. Pawde, R. Mapari, V. Patil, D. Pawar (2024) Anisotropic behavior of universe in $f(R, L_m)$ gravity with varying deceleration parameter. *Eur. Phys. J. C* **84**(3) 320.
- [77] T. Harko, F.S. Lobo (2014) Generalized curvature-matter couplings in modified gravity. *Galaxies* **2**(3) 410-465.
- [78] T. Harko, F.S. Lobo, J.P. Mimoso, D. Pavón (2015) Gravitational induced particle production through a nonminimal curvature-matter coupling. *Eur. Phys. J. C* **75**(8) 386.
- [79] C. Chawla, R. Mishra, A. Pradhan (2012) String cosmological models from early deceleration to current acceleration phase with varying G and Λ . *Eur. Phys. J. Plus* **127**(11) 137.
- [80] M. Koussour, M. Bennai (2023) Anisotropic background for two fluids: Matter and holographic dark energy. *J. Astrophys. Astron.* **44**(1) 6.
- [81] R. Nagpal, J. Singh, A. Beesham, H. Shabani (2019) Cosmological aspects of a hyperbolic solution in $f(R, T)$ gravity. *Annals of Phys.(NY)* **405** 234-255.
- [82] G. Sharov, V. Vasiliev (2018) How predictions of cosmological models depend on Hubble parameter data sets *arXiv preprint arXiv:1807.07323*.
- [83] D. Brout, D. Scolnic, B. Popovic, A.G. Riess, A. Carr, J. Zuntz, R. Kessler, T.M. Davis, S. Hinton, D. Jones, et al. (2022) The pantheon analysis: cosmological constraints. *Astrophys. J.* **938**(2) 110.
- [84] M. Koussour, A. Errehymy, O. Donmez, K. Myrzakulov, M. Khan, B. Çil, E. Güdekli (2024) Constraints on bulk viscosity in $f(Q, T)$ gravity from $H(z)$ /pantheon+ data. *Phys. Dark Universe* **45** 101527.
- [85] M. Kowalski, D. Rubin, G. Aldering, R. Agostinho, A. Amadon, R. Amanullah, C. Balland, K. Barbary, G. Blanc, P.J. Challis, et al. (2008) Improved cosmological constraints from new, old, and combined supernova data sets. *Astrophys. J.* **686**(2) 749.
- [86] R. Amanullah, C. Lidman, D. Rubin, G. Aldering, P. Astier, K. Barbary, M. Burns, A. Conley, K. Dawson, S. Deustua, et al. (2010) Spectra and Hubble space telescope light curves of six type ia supernovae at $0.511 < z < 1.12$ and the Union2 compilation. *Astrophys. J.* **716**(1) 712.
- [87] N. Suzuki, D. Rubin, C. Lidman, G. Aldering, R. Amanullah, K. Barbary, L. Barrientos, J. Botyanszki, M. Brodwin, N. Connolly, et al. (2012) The Hubble space telescope cluster supernova survey. V. Improving the dark-energy constraints above $z > 1$ and building an early-type-hosted supernova sample. *Astrophys. J.* **746**(1) 85.
- [88] M. Betoule, R. Kessler, J. Guy, J. Mosher, D. Hardin, R. Biswas, P. Astier, P. El-Hage, M. König, S. Kuhlmann, et al. (2014) Improved cosmological constraints from a joint analysis of the SDSS-II and SNLS supernova samples. *Astron. Astrophys.* **568** A22.

- [89] D.M. Scolnic, D. Jones, A. Rest, Y. Pan, R. Chornock, R. Foley, M. Huber, R. Kessler, G. Narayan, A. Riess, et al. (2018) The complete light-curve sample of spectroscopically confirmed SNe ia from Pan-STARRS1 and cosmological constraints from the combined pantheon sample. *Astrophys. J.* **859**(2) 101.
- [90] J.D. Barrow (2020) The area of a rough black hole. *Phys. Lett. B* **808** 135643.
- [91] S. Wang, Y. Wang, M. Li (2017) Holographic dark energy. *Phys. Rep.* **696** 1-57.
- [92] M. Yarahmadi (2025) Barrow interacting holographic dark energy cosmology with Hubble horizon as IR cutoff: A model can alleviating the Hubble and S_8 tension. *Phys. Dark Universe* **47** 101733.
- [93] A. Kotal, U. Debnath, A. Pradhan (2025) Cosmological parameter analysis and correspondence of $f(R)$, $f(G)$, $f(T)$ gravity models within the (m, n) -type Barrow holographic dark energy framework. *Phys. Scr.* **100** 115302.
- [94] N. Myrzakulov, S. Shekh, A. Pradhan (2025) Probing dark energy properties with Barrow holographic model in $f(Q, C)$ gravity. *Phys. Dark Universe* **47** 101790.
- [95] S. Bhojar, A. Pawar, Y.B. Ingole, S. Singhal: Bianchi type VI₀ cosmological model in context of holographic dark energy in $f(T)$ gravity.
- [96] C. Gao, F. Wu, X. Chen, Y.-G. Shen (2009) Holographic dark energy model from ricci scalar curvature *Phys. Rev. D* **79**(4) 043511.
- [97] S. Nojiri, S.D. Odintsov (2006) Unifying phantom inflation with late-time acceleration: Scalar phantom-non-phantom transition model and generalized holographic dark energy. *Gen. Relativ. Gravit.* **38**(8) 1285-1304.
- [98] L. Xu, J. Lu, W. Li (2009) Generalized holographic and Ricci dark energy models. *Eur. Phys. J. C* **64**(1) 89-95.
- [99] U.K. Sharma, V. Srivastava (2021) Tsallis HDE with an IR cutoff as Ricci horizon in a flat FLRW universe. *New Astronomy* **84** 101519.
- [100] Z. Feizi Mangoudehi (2022) Observational constraints on Tsallis holographic dark energy with Ricci horizon cutoff. *Astrophys. Space Sci.* **367**(12) 115.
- [101] M.-H. Belkacemi, M. Bouhmadi-López, A. Errahmani, T. Quali (2012) Holographic induced gravity model with a Ricci dark energy: Smoothing the little rip and big rip through Gauss-Bonnet effects. *Phys. Rev. D* **85**(8) 083503.
- [102] N. Mazumder, R. Biswas, S. Chakraborty (2011) Interacting holographic dark energy at the Ricci scale and dynamical system. [arXiv preprint arXiv:1106.4627](https://arxiv.org/abs/1106.4627).
- [103] L.P. Chimento, M.G. Richarte (2011) Interacting dark matter and modified holographic Ricci dark energy induce a relaxed Chaplygin gas. *Phys. Rev. D* **84**(12) 123507.
- [104] D. Pawar, R. Mapari, P. Agrawal (2019) A modified holographic ricci dark energy model in $f(R, T)$ theory of gravity. *J. Astrophys. Astron.* **40**(2) 13.
- [105] A. Shaikh, A. Shaikh, K. Wankhade (2019) Hypersurface-homogeneous modified holographic Ricci dark energy cosmological model by hybrid expansion law in Saez-Ballester theory of gravitation. *J. Astrophys. Astron.* **40**(3) 25.
- [106] A. Raychaudhuri (1955) Relativistic cosmology. I. *Phys. Rev.* **98**(4) 1123.
- [107] S. Mandal, P. Sahoo, J.R. Santos (2020) Energy conditions in $f(Q)$ gravity. *Phys. Rev. D* **102**(2) 024057.
- [108] Y. Xu, G. Li, T. Harko, S.-D. Liang (2019) $f(Q, T)$ gravity. *Eur. Phys. J. C* **79** 708.